Dynamics of formation and interaction of photorefractive screening solitons

C. Denz, W. Królikowski,* J. Petter, C. Weilnau, and T. Tschudi
Light- and Particle Optics Group, Institute of Applied Physics, Darmstadt University of Technology, Hochschulstrasse 6, D-64289 Darmstadt, Germany

M. R. Belić,† F. Kaiser, and A. Stepken
Theoretical Nonlinear Dynamics Group, Institute of Applied Physics, Darmstadt University of Technology, Hochschulstrasse 4a, D-64289 Darmstadt, Germany

(Received 28 December 1998)

An experimental and numerical investigation of the dynamical, time-dependent effects accompanying the formation and interaction of two-dimensional spatial screening solitons in a photorefractive strontium barium niobate crystal is performed. These effects include initial diffraction, collapse to the soliton shape, the oscillation of beam diameters, beam bending, and the rotation, twisting, and turning of soliton pairs. The dynamics of complex spiraling of two incoherent solitons is considered in more detail. [S1063-651X(99)05611-1]

PACS number(s): 42.65.Tg, 42.65.Hw, 42.65.Jx

Spatial optical solitons have been the subject of considerable interest in the past decades. They occur when the diffraction of a light beam during propagation is exactly balanced by the nonlinear self-focusing effect in the material. Among others, photorefractive screening solitons can be created at extremely low laser powers using a biasing dc electric field and a background illumination [1–4]. The simplicity of the generation makes them attractive for applications in all-optical beam guiding, switching and logic operations [5–8]. In addition, screening solitons present a useful tool in the experimental verification of theoretical predictions regarding their generic properties. Indeed, recent experiments with photorefractive (PR) crystals have led to the demonstration of effects as fusion [9,10], creation [11], annihilation [12], and spiraling [13] of spatial solitons.

All of these effects have been described theoretically mostly in steady-state situations. Even though time-dependent effects were readily observed, only a few theories included time from the onset [14]. In the case of effects concerning formation and especially interaction of two-dimensional (2D) spatial solitons, temporal effects become essential—a requirement that leads immediatedly to formidable theoretical and computational problems. We are not aware of numerical procedures that adequately treat the dynamics of 2D anisotropic spatial screening solitons and their interaction. Nonetheless, resolving the temporal development of soliton formation and interaction may shed some light on open questions as, e.g., soliton spiraling [15,16] and is the only way to obtain a complete insight in spatial soliton physics.

Our aim is twofold. First, we present experimental results displaying the anomalous anisotropic [17,18] dynamical behavior of the formation and interaction of incoherent PR screening solitons. Second, we explain this behavior in terms of a model that includes the temporal development of soliton formation. In particular, we focus our attention on a case where the initial launching conditions create complex interaction scenarios. We will elucidate the question of soliton spiraling, showing both experimentally and numerically how the two solitons wind in a complex manner until the beams are pinned to the attractive well created by the interaction of the biasing electic field and the photorefractive space charge field.

The formation and interaction of mutually incoherent spatial solitons was investigated experimentally in a standard configuration [11,12,18]. A cerium-doped strontium barium niobate (SBN) crystal was used as the PR material, having a size of $13.5\times5\times5$ mm^3 $(a\times b\times c)$. The crystal was biased with a dc voltage of 2–3 kV applied along its polar c axis (x axis of the coordinate system). One or two circular beams derived from a frequency-doubled Nd:YAG laser ($\lambda=532$ nm) were directed by a system of mirrors and beam splitters onto the entrance face (x,y) of the crystal. The relative angle of the interacting beams could be precisely adjusted by the external mirrors. The beams had Gaussian diameters of $\sim 15\mu$m, an intensity of 2–4 μW, and were polarized along the x axis to make use of the large r_{33} electro-optic coefficient. One of the beams was phase-modulated by reflection from a mirror mounted on a piezoelectric transducer. Driving the transducer by an ac voltage at several hundred Hertz makes the beams effectively incoherent due to the slow response of the PR medium. The process of soliton formation was always accompanied by self-bending of the soliton's trajectory (several tens of μm, depending on the propagation length). It results from a nonlocal contribution to the nonlinear refractive index change [19–21] due to the diffusion of photoexcited charges and increases when reducing the beam diameter.

The PR nonlinearity has a saturable character. The process of screening is determined by the degree of saturation, which is defined as the ratio of the soliton peak intensity to background illumination. To control the saturation, the crystal was illuminated by a wide beam derived from a white

*Permanent adress: Australian Photonics Cooperative Research Center, Laser Physics Center, Australian National University, Canberra ACT 0200, Australia.

†Permanent address: Institute of Physics, P.O. Box 57, 11001 Belgrade, Yugoslavia.

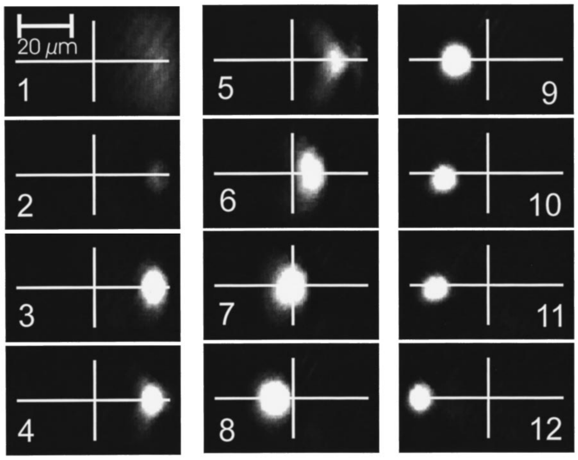

FIG. 1. Formation and dynamics of a single soliton of the crystal. The time interval between consecutive frames is 0.5 s, frame 12 shows the steady state 7.5 s after launching the beam.

light source, giving a saturation level of about 2 for all beams. With these parameters the beams would always form elliptically shaped solitons with a diameter ratio of 1:1.2 ($w_x \approx 10\,\mu$m wide along the x axis), when propagating individually.

Experimental results are given in Figs. 1–3, where we show the output light intensity distributions of a single soliton and a soliton pair at different times, seen at the exit face of the crystal. In all our results, the x axis is horizontal and the external field points to the left. A Gaussian beam launched into the crystal is initially diffracted while propagating through the crystal bulk (Fig. 1.1). During the first second, the beam is strongly focused to its elliptical shape. Within the next seconds [Figs. 1.4–1.11], the beam starts bending in the direction of the electric field, as it is known from steady-state investigations. However, a closer look at the temporally resolved representation reveals that the beam experiences transient oscillations in its diameter, which may result for a short time period in almost a doubling of the former beam diameter. Figure 1.12 shows the steady state after 7.5 s, where the bending distance is nearly five times the diameter ($d \approx 55\,\mu$m) of the beam.

When two incoherent screening solitons are launched into the PR medium, they exhibit a complex interaction behavior due to the inherent anisotropy of their common potential [18,22]. Domains of attraction and repulsion in the transverse plane may lead to the mutual rotation of the beams, spiraling of soliton trajectories, or to a wobbling of the center of mass of two solitons. In the following, we will restrict our analysis to the case of soliton interaction where both beams

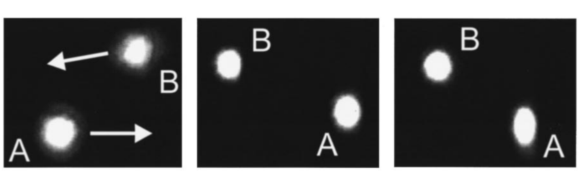

FIG. 2. Rotation of a soliton pair. (a) Beams at the entrance face of the crystal, indicating the direction of skewing of both beams. Steady-state situation at the exit face (b) without and (c) with interaction. The pictures have been corrected to remove the displacement along the x axis due to bending.

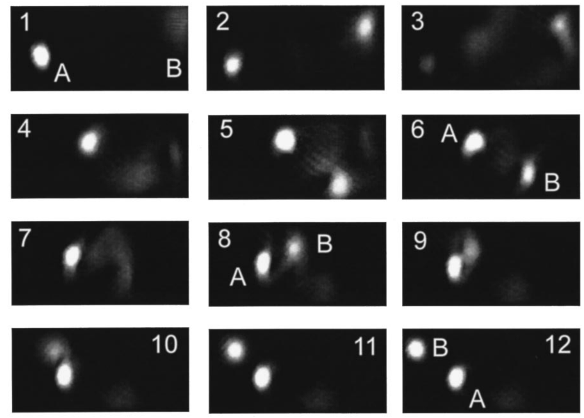

FIG. 3. Time-resolved complex rotation of a soliton pair. The sequence starts when a second beam is launched onto a steady-state soliton. The time interval between consecutive frames is 0.36 s.

are launched skewed to each other into the nonlinear medium, thus creating a complex spiraling behavior. We will show that our time-resolved analysis may clarify the question, under which conditions different spiraling angles can be achieved in PR screening soliton interaction. Recently, a tricky experimental arrangement was used to record full, DNA-like spiraling [13] in the steady-state representation.

In Fig. 2, a typical interaction situation is depicted in a steady-state configuration. The first image [Fig. 2(a)] shows the intensity distribution of the input beams, where beam A has a slightly higher intensity than beam B. They are separated along an axis tilted at $\approx 44°$ with respect to the x axis, having a symmetric initial angular momentum of 0.4° in the x direction and an asymmetric one of 0.1° (beam B) in the y direction. Figures 2(b) and 2(c) contain output intensity distributions for noninteracting (independent propagation) and interacting solitons, respectively. The figure shows that for this particular case the mutual interaction results not only in attraction and repulsion, but also in a motion about the center of the beams. It can be interpreted as a small rotation of several degrees or a rotation of almost 2π.

When this situation is resolved in time, the insight into the interaction behavior becomes much more transparent. The experimental results shown in Fig. 3 were realized forming a steady-state two-beam interaction configuration, and then blocking and unblocking one of the interaction beams. By this means, the temporal evolution of the interaction can be much more clearly visualized than in the case of simultaneous formation. Moreover, the identification of each beam during the temporal evolution can be ensured at each time step by blocking one of the beams. The sequence starts when a single beam has reached steady state. Unblocking the second beam first leads to the formation of the soliton beam at its launching position (Fig. 3.2). Subsequently, both beams break up into different spatial components (Fig. 3.3), until they reappear in a clockwise rotated position (Fig. 3.6). Then beam B rotates counter-clockwise around beam A, and reaches its steady-state position (Figs. 3.7–3.12). Note that the solitons turn around each other in an elliptical orbit, as was found in [13].

The model describing the interaction of screening solitons in PR media is based on the paraxial approximation to the propagation of optical beams and the Kukhtarev material equations [17,22]. The propagation of beams along the z axis is described by the following equations:

$$\left[\frac{\partial}{\partial z}+\boldsymbol{\theta}_1\cdot\boldsymbol{\nabla}-\frac{i}{2}\nabla^2\right]A_1=\frac{i\gamma}{2}\left(\frac{\partial\varphi}{\partial x}-E_0\right)A_1, \tag{1a}$$

$$\left[\frac{\partial}{\partial z}+\boldsymbol{\theta}_2\cdot\boldsymbol{\nabla}-\frac{i}{2}\nabla^2\right]A_2=\frac{i\gamma}{2}\left(\frac{\partial\varphi}{\partial x}-E_0\right)A_2 \tag{1b}$$

for the slowly varying envelopes of the two beams $A_1(\mathbf{r})$ and $A_2(\mathbf{r})$. The vectors $\boldsymbol{\theta}_1$ and $\boldsymbol{\theta}_2$ specify the directions of beam launching, $\boldsymbol{\nabla}$ is the transverse gradient, and $\gamma=k^2n^4w^2r_{\mathrm{eff}}$ is the medium-light coupling constant. Here k is the wave number of light, n is the index of refraction, w is the initial beam spot size, and r_{eff} is the effective element of the electro-optic tensor. The transverse coordinates x and y are scaled by w and the propagation coordinate z is scaled by the diffraction length $L_D=knw^2$. φ is the electrostatic potential induced by the light, whose evolution is described by the following, time-dependent relaxation equation

$$\tau\frac{\partial}{\partial t}(\nabla^2\varphi)+\nabla^2\varphi+\boldsymbol{\nabla}\varphi\cdot\boldsymbol{\nabla}\ln I$$
$$=E_0\frac{\partial}{\partial x}\ln I+\frac{k_BT}{e}[\boldsymbol{\nabla}^2\ln I+(\boldsymbol{\nabla}\ln I)^2], \tag{2}$$

where τ is the relaxation time of the crystal and E_0 is the external field. The normalized intensity $I=1+|A_1|^2+|A_2|^2$ is measured in units of the saturation intensity. The terms on the right side of Eq. (2) describe the drift and diffusion of charges in the crystal. The set of Eqs. (1) and (2) is integrated numerically by spectral methods for a range of initial conditions that is close to the experimental situation described above. Since the SBN crystal is rather slow (the relaxation time τ is on the order of seconds), the dynamics of the beams is slaved to the crystal. Therefore, all temporal changes stem from the potential equation and the propagation of the beams can be separated from and nested within the temporal integration loop.

The formation of a soliton, as seen in our numerical simulation, is presented in Fig. 4. Fig. 4(a) shows the temporal evolution when diffusion is neglected as a contribution in the soliton formation process. The initial normalized intensity of the beam is 5, and its initial diameter is $w=15\,\mu$m. Pronounced oscillations of the x diameter of the beam can be found. After $t\approx 8\tau$ the beam reaches its steady state. These initial oscillations are less distinct for beams of lower intensity and smaller width. The reason for the oscillation is the symmetric nature of the Gaussian beam launched into the crystal, on the one hand, and the asymmetric nature of the screening on the other. Therefore, a beam needs a certain time to settle into a spatial soliton shape. If a beam with an exact spatial soliton shape could be launched into the crystal, this transient oscillating phase would be shortened. In Fig. 4(b), the diffusion of the charge carriers is considered. To reduce the transient oscillations, the initial intensity is reduced to 1.5, and the beam diameter is chosen to be $w=12\,\mu$m. The stages in the formation qualitatively follow the stages visible in the experimental development, as presented in Fig. 1: first diffraction of the beam, followed by focusing and bending until the steady state is reached.

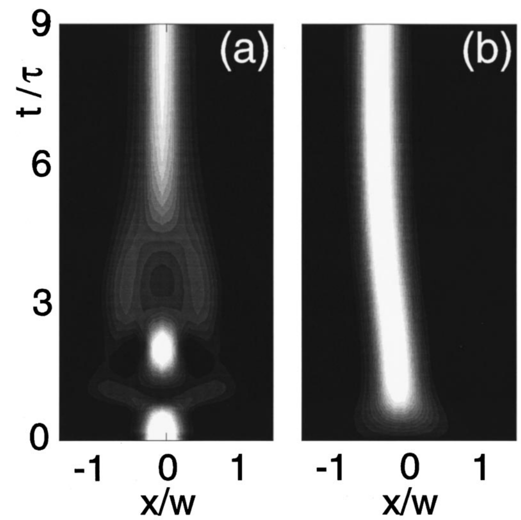

FIG. 4. Formation of a soliton beam; numerical simulation. Temporal evolution across the beam at the exit face for a case with (a) negligible diffusion contribution and (b) diffusion contribution. The beams propagate for 3.4 mm.

For the case of interacting solitons, the launching of skewed beams at higher intensities offers the possibility of prolonged spiraling. A numerical example is presented in

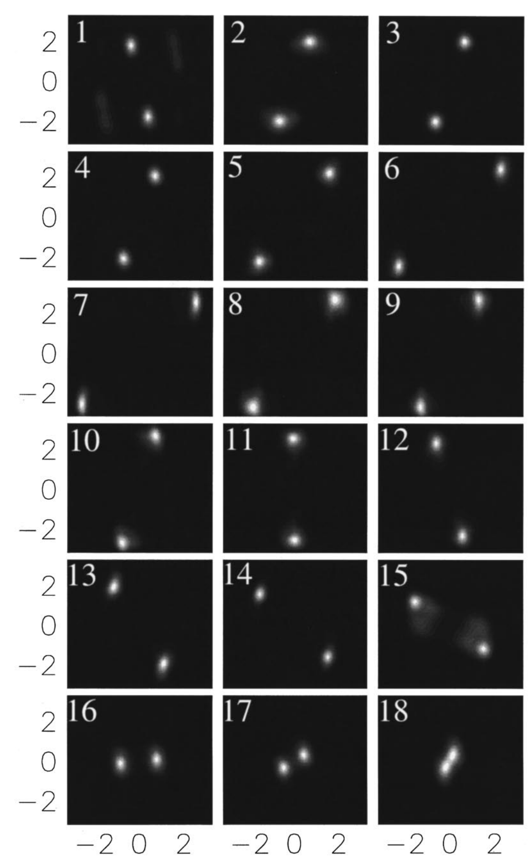

FIG. 5. Dynamical spiraling of a pair of solitons at the exit face; numerical. The intensity of the beams is 5 and the initial tilt is ∓ 0.8 and ∓ 0.2 relative to the transverse axes. The first frame is taken at $t=3\tau$, subsequent frames at $\Delta t=0.3\tau$.

Fig. 5, where tilted beams carrying an initial angular momentum relative to the origin are interacting. The trajectories observed are not simple, smooth spirals. The relative distance of the beams oscillates while spiraling. The potential in which the solitons rotate is not central. The attractive well along the y axis and the repulsive region along the x axis break the symmetry and prevent indefinite spiraling. The beams in Fig. 5 are initially set on a course that brings them to a close proximity. When the solitons are close to each other and interact strongly, they entangle and their individual identities are questionable. The light intensity distributions do not show two distinct spots. Nonetheless, the two bright spots reappear as the beams disentangle. We chose to present numerically the case of two high-intensity well-separated solitons that form two distinct bright spots as they interact. The sequence starts at $t=3\tau$, as the solitons disentangle after the initial close encounter. In the beginning (Fig. 5.1–5.7) they rotate clockwise, then reverse the sense of rotation to produce an oscillation around the y axis. Afterwards, counterclockwise spiraling continues for more than 300 degrees (Figs. 5.8–5.18) before the solitons freeze approximately along the y axis. The rotation does not proceed uniformly, i.e., at Fig. 5.15 it speeds up, so that between Fig. 5.14 and Fig. 5.16 the beams spiral for more than 180°. Note that the change in the rotation sense and a nonuniform rotation are also observed in the experiment shown in Fig. 3. Although the difference between the two cases is that the experiment is performed for less intense beams at a different separation distance, most of the important features of the spiraling interaction are present in experiment and theory. Therefore, temporally resolving the behavior gives insight into the complex interaction scenarios that take place during soliton propagation. Especially, effects of oscillations of the beam diameter and the beam separation distance as well as different speeds of the rotational motion can be identified.

In summary, we have investigated the dynamics of formation and spiraling of 2D screening solitons in a PR SBN crystal. Both experimental investigation and numerical simulations of a theoretical model have been performed in a time-resolved fashion. They provide insight into the details of soliton formation and interaction, having qualitatively consistent results. The special case of off-axis launching of two beams in combination with an initial angular tilt results in a complicated motion of the solitons in the transverse plane which are rotating about each other, twisting and turning in the region of attraction.

This work was partially supported by the Deutsche Forschungsgemeinschaft, SFB 185 ''Nonlinear Dynamics.''

[1] M. D. Iturbe-Castillo, P. A. Marquez-Aguilar, J. J. Sanchez-Mondragon, S. Stepanov, and V. Vysloukh, Appl. Phys. Lett. **64**, 408 (1994).

[2] M. Segev, G. C. Valley, B. Crosignani, P. DiPorto, and A. Yariv, Phys. Rev. Lett. **73**, 3211 (1994); D. N. Christodoulides and M. I. Carvalho, J. Opt. Soc. Am. B **12**, 1628 (1995).

[3] M. Shih, M. Segev, G. C. Valley, G. Salamo, B. Crosignani, and P. DiPorto, Electron. Lett. **31**, 826 (1995).

[4] A. A. Zozulya, D. Z. Anderson, A. V. Mamaev, and M. Saffman, Europhys. Lett. **36**, 419 (1996).

[5] T.-T. Shi, S. Chi, Opt. Lett. **15**, 1123 (1990); R. McLeod, K. Wagner, and S. Blair, Phys. Rev. A **52**, 3254 (1995); P. D. Miller and N. N. Akhmediev, Phys. Rev. E **53**, 4098 (1996).

[6] B. Luther-Davies and X. Yang, Opt. Lett. **17**, 498 (1992); B. Luther-Davies, X. Yang, and W. Krolikowski, Int. J. Nonlinear Opt. Phys. **2**, 339 (1993).

[7] W. J. Firth, A. J. Scroggie, Phys. Rev. Lett. **76**, 1623 (1996); M. Brambilla, L. A. Lugiato, and M. Stefani, Europhys. Lett. **34**, 109 (1996).

[8] R. de la Fuente, A. Barthelemy, and C. Froehly, Opt. Lett. **16**, 793 (1991).

[9] M. Shih and M. Segev, Opt. Lett. **21**, 1538 (1996).

[10] M. Shih, M. Segev, and G. Salamo, Appl. Phys. Lett. **69**, 4151 (1996).

[11] W. Królikowski and S. A. Holmstrom, Opt. Lett. **22**, 369 (1997).

[12] W. Krolikowski, B. Luther-Davies, C. Denz, and T. Tschudi, Opt. Lett. **23**, 97 (1998).

[13] M. Shih, M. Segev, and G. Salamo, Phys. Rev. Lett. **78**, 2551 (1997).

[14] A. A. Zozulya and D. Z. Anderson, Phys. Rev. A **51**, 1520 (1995); N. Fressengeas, J. Maufoy, and G. Kugel, Phys. Rev. E **54**, 6866 (1996); P. A. Marquez Aguilar, J. J. Sanchez-Mondragon, S. Stepanov, and V. Vysloukh, Phys. Rev. A **54**, R2563 (1996); B. Crosignani, P. DiPorto, A. Degasperis, M. Segev, and S. Trillo, J. Opt. Soc. Am. B **14**, 3078 (1997).

[15] A. Stepken, M. R. Belic, F. Kaiser, W. Krolikowski, and B. Luther-Davies, Phys. Rev. Lett. **82**, 540 (1999).

[16] M. R. Belic, A. Stepken, and F. Kaiser, Phys. Rev. Lett. **82**, 544 (1999).

[17] A. A. Zozulya and D. Z. Anderson, Phys. Rev. A **51**, 1520 (1995).

[18] W. Krolikowski, M. Saffman, B. Luther-Davies, and C. Denz, Phys. Rev. Lett. **80**, 3240 (1998).

[19] M. Shih, M. Segev, G. C. Valley, G. Salamo, B. Crosignani, and P. DiPorto, Electron. Lett. **31**, 826 (1995).

[20] M. I. Carvalho, S. R. Singh, and D. N. Christodoulides, Opt. Commun. **120**, 311 (1995).

[21] W. Krolikowski, N. Akhmediev, B. Luther-Davies, and M. Cronin-Golomb, Phys. Rev. E **54**, 5761 (1996).

[22] A. Stepken, F. Kaiser, M. R. Belić, and W. Krolikowski, Phys. Rev. E **58**, R4112 (1998).